

## Measurements of the observed cross sections for $e^+e^- \rightarrow$ light hadrons at $\sqrt{s} = 3.773$ and 3.650 GeV

M. Ablikim<sup>1</sup>, J. Z. Bai<sup>1</sup>, Y. Ban<sup>12</sup>, X. Cai<sup>1</sup>, H. F. Chen<sup>16</sup>, H. S. Chen<sup>1</sup>, H. X. Chen<sup>1</sup>, J. C. Chen<sup>1</sup>, Jin Chen<sup>1</sup>, Y. B. Chen<sup>1</sup>, Y. P. Chu<sup>1</sup>, Y. S. Dai<sup>18</sup>, L. Y. Diao<sup>9</sup>, Z. Y. Deng<sup>1</sup>, Q. F. Dong<sup>15</sup>, S. X. Du<sup>1</sup>, J. Fang<sup>1</sup>, S. S. Fang<sup>1a</sup>, C. D. Fu<sup>15</sup>, C. S. Gao<sup>1</sup>, Y. N. Gao<sup>15</sup>, S. D. Gu<sup>1</sup>, Y. T. Gu<sup>4</sup>, Y. N. Guo<sup>1</sup>, K. L. He<sup>1</sup>, M. He<sup>13</sup>, Y. K. Heng<sup>1</sup>, J. Hou<sup>11</sup>, H. M. Hu<sup>1</sup>, J. H. Hu<sup>3</sup>, T. Hu<sup>1</sup>, X. T. Huang<sup>13</sup>, X. B. Ji<sup>1</sup>, X. S. Jiang<sup>1</sup>, X. Y. Jiang<sup>5</sup>, J. B. Jiao<sup>13</sup>, D. P. Jin<sup>1</sup>, S. Jin<sup>1</sup>, Y. F. Lai<sup>1</sup>, G. Li<sup>1c</sup>, H. B. Li<sup>1</sup>, J. Li<sup>1</sup>, R. Y. Li<sup>1</sup>, S. M. Li<sup>1</sup>, W. D. Li<sup>1</sup>, W. G. Li<sup>1</sup>, X. L. Li<sup>1</sup>, X. N. Li<sup>1</sup>, X. Q. Li<sup>11</sup>, Y. F. Liang<sup>14</sup>, H. B. Liao<sup>1</sup>, B. J. Liu<sup>1</sup>, C. X. Liu<sup>1</sup>, F. Liu<sup>6</sup>, Fang Liu<sup>1</sup>, H. H. Liu<sup>1</sup>, H. M. Liu<sup>1</sup>, J. Liu<sup>12d</sup>, J. B. Liu<sup>1</sup>, J. P. Liu<sup>17</sup>, Jian Liu<sup>1</sup>, Q. Liu<sup>1</sup>, R. G. Liu<sup>1</sup>, Z. A. Liu<sup>1</sup>, Y. C. Lou<sup>5</sup>, F. Lu<sup>1</sup>, G. R. Lu<sup>5</sup>, J. G. Lu<sup>1</sup>, C. L. Luo<sup>10</sup>, F. C. Ma<sup>9</sup>, H. L. Ma<sup>2</sup>, L. L. Ma<sup>1e</sup>, Q. M. Ma<sup>1</sup>, Z. P. Mao<sup>1</sup>, X. H. Mo<sup>1</sup>, J. Nie<sup>1</sup>, R. G. Ping<sup>1</sup>, N. D. Qi<sup>1</sup>, H. Qin<sup>1</sup>, J. F. Qiu<sup>1</sup>, Z. Y. Ren<sup>1</sup>, G. Rong<sup>1</sup>, X. D. Ruan<sup>4</sup>, L. Y. Shan<sup>1</sup>, L. Shang<sup>1</sup>, C. P. Shen<sup>1</sup>, D. L. Shen<sup>1</sup>, X. Y. Shen<sup>1</sup>, H. Y. Sheng<sup>1</sup>, H. S. Sun<sup>1</sup>, S. S. Sun<sup>1</sup>, Y. Z. Sun<sup>1</sup>, Z. J. Sun<sup>1</sup>, X. Tang<sup>1</sup>, G. L. Tong<sup>1</sup>, D. Y. Wang<sup>1f</sup>, L. Wang<sup>1</sup>, L. L. Wang<sup>1</sup>, L. S. Wang<sup>1</sup>, M. Wang<sup>1</sup>, P. Wang<sup>1</sup>, P. L. Wang<sup>1</sup>, Y. F. Wang<sup>1</sup>, Z. Wang<sup>1</sup>, Z. Y. Wang<sup>1</sup>, Zheng Wang<sup>1</sup>, C. L. Wei<sup>1</sup>, D. H. Wei<sup>1</sup>, Y. Weng<sup>1</sup>, N. Wu<sup>1</sup>, X. M. Xia<sup>1</sup>, X. X. Xie<sup>1</sup>, G. F. Xu<sup>1</sup>, X. P. Xu<sup>6</sup>, Y. Xu<sup>11</sup>, M. L. Yan<sup>16</sup>, H. X. Yang<sup>1</sup>, Y. X. Yang<sup>3</sup>, M. H. Ye<sup>2</sup>, Y. X. Ye<sup>16</sup>, G. W. Yu<sup>1</sup>, C. Z. Yuan<sup>1</sup>, Y. Yuan<sup>1</sup>, S. L. Zang<sup>1</sup>, Y. Zeng<sup>7</sup>, B. X. Zhang<sup>1</sup>, B. Y. Zhang<sup>1</sup>, C. C. Zhang<sup>1</sup>, D. H. Zhang<sup>1</sup>, H. Q. Zhang<sup>1</sup>, H. Y. Zhang<sup>1</sup>, J. W. Zhang<sup>1</sup>, J. Y. Zhang<sup>1</sup>, S. H. Zhang<sup>1</sup>, X. Y. Zhang<sup>13</sup>, Yiyun Zhang<sup>14</sup>, Z. X. Zhang<sup>12</sup>, Z. P. Zhang<sup>16</sup>, D. X. Zhao<sup>1</sup>, J. W. Zhao<sup>1</sup>, M. G. Zhao<sup>1</sup>, P. P. Zhao<sup>1</sup>, W. R. Zhao<sup>1</sup>, Z. G. Zhao<sup>1g</sup>, H. Q. Zheng<sup>12</sup>, J. P. Zheng<sup>1</sup>, Z. P. Zheng<sup>1</sup>, L. Zhou<sup>1</sup>, K. J. Zhu<sup>1</sup>, Q. M. Zhu<sup>1</sup>, Y. C. Zhu<sup>1</sup>, Y. S. Zhu<sup>1</sup>, Z. A. Zhu<sup>1</sup>, B. A. Zhuang<sup>1</sup>, X. A. Zhuang<sup>1</sup>, B. S. Zou<sup>1</sup>

(BES Collaboration)

<sup>1</sup> Institute of High Energy Physics, Beijing 100049, People's Republic of China

<sup>2</sup> China Center for Advanced Science and Technology (CCAST), Beijing 100080, People's Republic of China

<sup>3</sup> Guangxi Normal University, Guilin 541004, People's Republic of China

<sup>4</sup> Guangxi University, Nanning 530004, People's Republic of China

<sup>5</sup> Henan Normal University, Xinxiang 453002, People's Republic of China

<sup>6</sup> Huazhong Normal University, Wuhan 430079, People's Republic of China

<sup>7</sup> Hunan University, Changsha 410082, People's Republic of China

<sup>8</sup> Jinan University, Jinan 250022, People's Republic of China

<sup>9</sup> Liaoning University, Shenyang 110036, People's Republic of China

<sup>10</sup> Nanjing Normal University, Nanjing 210097, People's Republic of China

<sup>11</sup> Nankai University, Tianjin 300071, People's Republic of China

<sup>12</sup> Peking University, Beijing 100871, People's Republic of China

<sup>13</sup> Shandong University, Jinan 250100, People's Republic of China

<sup>14</sup> Sichuan University, Chengdu 610064, People's Republic of China

<sup>15</sup> Tsinghua University, Beijing 100084, People's Republic of China

<sup>16</sup> University of Science and Technology of China, Hefei 230026, People's Republic of China

<sup>17</sup> Wuhan University, Wuhan 430072, People's Republic of China

<sup>18</sup> Zhejiang University, Hangzhou 310028, People's Republic of China

<sup>a</sup> Current address: DESY, D-22607, Hamburg, Germany

<sup>b</sup> Current address: Johns Hopkins University, Baltimore, MD 21218, USA

<sup>c</sup> Current address: Universite Paris XI, LAL-Bat. 208- -BP34, 91898- ORSAY Cedex, France

<sup>d</sup> Current address: Max-Planck-Institut fuer Physik, Foehringer Ring 6, 80805 Munich, Germany

<sup>e</sup> Current address: University of Toronto, Toronto M5S 1A7, Canada

<sup>f</sup> Current address: CERN, CH-1211 Geneva 23, Switzerland

<sup>g</sup> Current address: University of Michigan, Ann Arbor, MI 48109, USA

Using the data sets of  $17.3 \text{ pb}^{-1}$  collected at  $\sqrt{s} = 3.773 \text{ GeV}$  and  $6.5 \text{ pb}^{-1}$  collected at  $\sqrt{s} = 3.650 \text{ GeV}$  with the BESII detector at the BEPC collider, we have measured the observed cross sections for 18 exclusive light hadron final states produced in  $e^+e^-$  annihilation at the two energy points.

## I. INTRODUCTION

The  $\psi(3770)$  resonance is the lowest mass charmonium resonance above the open charm pair  $D\bar{D}$  production threshold. It is expected to decay almost entirely into pure  $D\bar{D}$  [1]. However, it is difficult to understand for a long time that the observed cross section  $\sigma_{D\bar{D}}^{\text{obs}}$  for  $D\bar{D}$  production at the peak of  $\psi(3770)$  resonance is less than the observed cross section  $\sigma_{\psi(3770)}^{\text{obs}}$  for  $\psi(3770)$  production [2, 3]. Recently, BES Collaboration directly measured the branching fraction for  $\psi(3770) \rightarrow \text{non-}D\bar{D}$  to be  $(16.1 \pm 1.6 \pm 5.7)\%$  [4] and  $(16.4 \pm 7.3 \pm 4.7)\%$  [5] with two different data samples and different methods. These imply that the  $\psi(3770)$  might substantially decay into non- $D\bar{D}$  final states. However, the existing results about exclusive non- $D\bar{D}$  decays of  $\psi(3770)$  from BES [6, 7, 8, 9] and CLEO [10, 11, 12, 13, 14, 15] Collaborations can not explain the discrepancy between the  $\sigma_{D\bar{D}}^{\text{obs}}$  and  $\sigma_{\psi(3770)}^{\text{obs}}$ . To understand the discrepancy, at the first step, one can directly compare the observed cross sections for  $e^+e^- \rightarrow$  light hadrons at the center-of-mass energies below 3.660 GeV and at 3.773 GeV, removing the contributions from  $J/\psi$  and  $\psi(3686)$  decays due to ISR returns as well as the contributions from  $D\bar{D}$  decays. These cross sections provide useful information to understand the mechanisms of the continuum light hadron production and helpful information to understand the discrepancy between the  $\sigma_{D\bar{D}}^{\text{obs}}$  and  $\sigma_{\psi(3770)}^{\text{obs}}$ .

In this Letter, we report measurements of the observed cross sections for the exclusive light hadron final states of  $\phi\pi^0$ ,  $\phi\eta$ ,  $2(\pi^+\pi^-)$ ,  $K^+K^-\pi^+\pi^-$ ,  $2(K^+K^-)$ ,  $p\bar{p}\pi^+\pi^-$ ,  $p\bar{p}K^+K^-$ ,  $3(\pi^+\pi^-)$ ,  $\phi\pi^+\pi^-$ ,  $\phi K^+K^-$ ,  $\phi p\bar{p}$ ,  $2(\pi^+\pi^-)\eta$ ,  $2(\pi^+\pi^-)\pi^0$ ,  $K^+K^-\pi^+\pi^-\pi^0$ ,  $2(K^+K^-)\pi^0$ ,  $p\bar{p}\pi^0$ ,  $p\bar{p}\pi^+\pi^-\pi^0$  and  $3(\pi^+\pi^-)\pi^0$  produced in  $e^+e^-$  annihilation at  $\sqrt{s} = 3.773$  and 3.650 GeV. The measurements are made by analyzing the data sets of  $17.3 \text{ pb}^{-1}$  collected at  $\sqrt{s} = 3.773$  GeV and  $6.5 \text{ pb}^{-1}$  collected at  $\sqrt{s} = 3.650$  GeV with the BESII detector at the BEPC collider. For convenience, we call the data sets taken at  $\sqrt{s} = 3.773$  GeV and  $\sqrt{s} = 3.650$  GeV to be the  $\psi(3770)$  resonance data and the continuum data in the Letter, respectively.

## II. BESII DETECTOR

The BESII is a conventional cylindrical magnetic detector that is described in detail in Refs. [16, 17]. A 12-layer Vertex Chamber (VC) surrounding a beryllium beam pipe provides input to event trigger, as well as coordinate information. A forty-layer main drift chamber (MDC) located just outside the VC yields precise measurements of charged particle trajectories with a solid angle coverage of 85% of  $4\pi$ ; it also provides ionization energy loss ( $dE/dx$ ) measurements for particle identification. Momentum resolution of  $1.7\%\sqrt{1+p^2}$  ( $p$  in GeV/c) and  $dE/dx$  resolution of 8.5% for Bhabha scat-

tering electrons are obtained for the data taken at  $\sqrt{s} = 3.773$  GeV. An array of 48 scintillation counters surrounding the MDC measures time of flight (TOF) of charged particles with a resolution of about 180 ps for electrons. Outside the TOF counters, a 12 radiation length, lead-gas barrel shower counter (BSC), operating in limited streamer mode, measures the energies of electrons and photons over 80% of the total solid angle with an energy resolution of  $\sigma_E/E = 0.22/\sqrt{E}$  ( $E$  in GeV) and spatial resolutions of  $\sigma_\phi = 7.9$  mrad and  $\sigma_Z = 2.3$  cm for electrons. A solenoidal magnet outside the BSC provides a 0.4 T magnetic field in the central tracking region of the detector. Three double-layer muon counters instrument the magnet flux return and serve to identify muons with momentum greater than 500 MeV/c. They cover 68% of the total solid angle.

## III. EVENT SELECTION

The exclusive light hadron final states mentioned above are reconstructed with the final states  $m(\pi^+\pi^-)n(K^+K^-)i(p\bar{p})j(\gamma\gamma)$  ( $m = 0, 1, 2, 3$ ;  $n = 0, 1, 2$ ;  $i = 0, 1$  and  $j = 0, 1$ ), respectively. The  $\phi$ ,  $\pi^0$  and  $\eta$  mesons are reconstructed through the decays  $\phi \rightarrow K^+K^-$ ,  $\pi^0 \rightarrow \gamma\gamma$  and  $\eta \rightarrow \gamma\gamma$ .

To select candidate events, it is first required that at least two charged tracks be well reconstructed in the MDC with good helix fits. In order to ensure the well-measured 3-momentum vectors and the reliability of the charged-particle identification, the polar angle  $\theta$  of each charged track must satisfy  $|\cos\theta| < 0.85$ . It is then required that each charged track originate from the interaction region defined by  $\sqrt{V_x^2 + V_y^2} < 2.0$  cm and  $|V_z| < 20.0$  cm, where  $V_x$ ,  $V_y$  and  $V_z$  are the closest approach of the charged track in the  $x$ ,  $y$  and  $z$  directions.

Charged particles are identified by using the  $dE/dx$  and TOF measurements, with which the combined confidence levels ( $CL_\pi$ ,  $CL_K$  and  $CL_p$ ) for pion, kaon and proton hypotheses are calculated. A pion candidate is required to have  $CL_\pi > 0.001$ . A kaon candidate is required to satisfy  $CL_K > CL_\pi$  in order to reduce misidentification. A proton candidate is required to have the ratio  $\frac{CL_p}{CL_\pi + CL_K + CL_p}$  greater than 0.6.

The photons are selected with the BSC measurements. It is required that the energy deposited of the photon candidate in the BSC be greater than 50 MeV, and the electromagnetic shower start in the first 5 readout layers. Moreover, the angle between the photon and the nearest charged track is required to be greater than  $22^\circ$  [18], and the opening angle between the direction of the shower development and the direction of the photon emission is required to be less than  $37^\circ$  [18].

For each final state, there may be several different charged and/or neutral track combinations satisfying the above selection criteria in an event. In order to improve mass resolution, each combination is subjected to

an energy-momentum conservation kinematic fit. Only those combinations with the kinematic fit probability greater than 1% are accepted. If more than one combination satisfies the selection criteria in an event, only the combination with the largest fit probability is retained.

For the final state  $2(\pi^+\pi^-)$ , the background events of  $(\gamma)J/\psi\pi^+\pi^-$  with  $J/\psi \rightarrow \mu^+\mu^-$  are vetoed by requiring that the invariant mass of any  $\pi^+\pi^-$  combination be less than  $3.00 \text{ GeV}/c^2$ .

For the final state  $K^+K^-\pi^+\pi^-$  (or  $K^+K^-\pi^+\pi^-\pi^0$ ), the events from  $D\bar{D}$  decays are excluded by rejecting the events in which the  $D^0$  and  $\bar{D}^0$  mesons can be reconstructed in the decay modes of  $D^0 \rightarrow K^-\pi^+$  and  $\bar{D}^0 \rightarrow K^+\pi^-$  (or  $\bar{D}^0 \rightarrow K^+\pi^-\pi^0$ , here charge conjugations are implied) [19].

#### IV. DATA ANALYSIS

In the following data analysis, the modes containing  $\phi$  and/or  $\pi^0/\eta$  mesons in the final states are studied by examining the spectra of the  $K^+K^-$  and/or  $\gamma\gamma$  invariant masses ( $M_{K^+K^-}$  and/or  $M_{\gamma\gamma}$ ), which are calculated with the fitted momentum vectors from the kinematic fit. In the  $K^+K^-$  (or  $\gamma\gamma$ ) invariant mass spectrum for those final states with a few accepted events, the region within the  $20 \text{ MeV}/c^2$  (or  $3\sigma_{M_{\gamma\gamma}}^{\pi^0/\eta}$ ) window around the  $\phi$  (or  $\pi^0/\eta$ ) nominal mass is taken as the  $\phi$  (or  $\pi^0/\eta$ ) signal region. Here,  $\sigma_{M_{\gamma\gamma}}^{\pi^0/\eta}$  is the standard deviation of the  $\gamma\gamma$  invariant mass spectrum determined by Monte Carlo simulation.

To study the modes without intermediate sub-resonance decays in the final states, we define a kinematic quantity of the scaled energy as  $E_{\text{msr}}/E_{\text{cm}}$ , where  $E_{\text{msr}}$  is the total measured energy of all the observed particles, and  $E_{\text{cm}}$  is the nominal center-of-mass energy.

##### A. Candidates for $e^+e^- \rightarrow \phi\pi^0$ and $e^+e^- \rightarrow \phi\eta$

The resulting scatter plots of  $M_{K^+K^-}$  versus  $M_{\gamma\gamma}$  for the selected  $K^+K^-\gamma\gamma$  events are shown in Fig. 1, where the hatched areas show the  $\phi\pi^0$  and  $\phi\eta$  signal regions, while the solid, dashed and dotted boundary lines represent the  $\phi$ ,  $\pi^0$  and  $\eta$  signal regions, respectively. In the  $\phi\pi^0$  ( $\phi\eta$ ) signal region in the figure, there is 0(1) and 0(0) signal event for the  $\phi\pi^0$  ( $\phi\eta$ ) final state observed from the  $\psi(3770)$  resonance data and the continuum data, respectively.

##### B. Candidates for $e^+e^- \rightarrow m(\pi^+\pi^-)n(K^+K^-)i(p\bar{p})$

Figure 2 shows the resulting  $E_{\text{msr}}/E_{\text{cm}}$  distributions, with each peak centered around unity correctly, from the selected  $m(\pi^+\pi^-)n(K^+K^-)i(p\bar{p})$  events for studying  $e^+e^- \rightarrow 2(\pi^+\pi^-)$ ,  $e^+e^- \rightarrow K^+K^-\pi^+\pi^-$ ,  $e^+e^- \rightarrow$

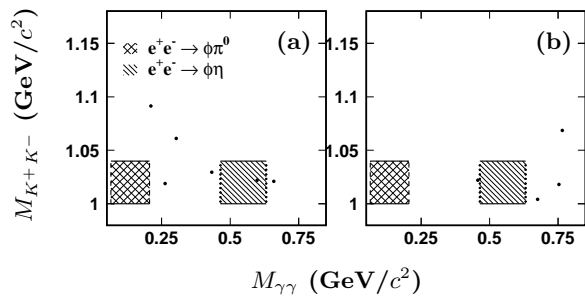


FIG. 1: The scatter plots of  $M_{K^+K^-}$  versus  $M_{\gamma\gamma}$  for the  $K^+K^-\gamma\gamma$  combinations selected from (a) the  $\psi(3770)$  resonance data and (b) the continuum data, where the hatched areas denote the  $\phi\pi^0$  and  $\phi\eta$  signal regions, while the solid, dashed and dotted boundary lines represent the  $\phi$ ,  $\pi^0$  and  $\eta$  signal regions, respectively.

$2(K^+K^-)$ ,  $e^+e^- \rightarrow p\bar{p}\pi^+\pi^-$ ,  $e^+e^- \rightarrow p\bar{p}K^+K^-$  and  $e^+e^- \rightarrow 3(\pi^+\pi^-)$ . Fitting to the spectrum with a Gaussian function for the signal and a flat background yields the number  $N^{\text{obs}}$  of the signal events for each mode observed from the  $\psi(3770)$  resonance data and the continuum data.

##### C. Candidates for $e^+e^- \rightarrow \phi K^+K^-$ , $e^+e^- \rightarrow \phi\pi^+\pi^-$ and $e^+e^- \rightarrow \phi p\bar{p}$

To investigate the processes  $e^+e^- \rightarrow \phi K^+K^-$ ,  $e^+e^- \rightarrow \phi\pi^+\pi^-$  and  $e^+e^- \rightarrow \phi p\bar{p}$ , we further analyze the  $K^+K^-$  invariant mass spectra of the selected  $2(K^+K^-)$ ,  $K^+K^-\pi^+\pi^-$  and  $p\bar{p}K^+K^-$  events, as shown in Fig. 3. The  $\phi$  signals can be seen in Figs. 3(a) and 3(a'). Fitting to these two  $K^+K^-$  invariant mass spectra with a Gaussian function for the  $\phi$  signal and a flat background yields  $12.1 \pm 5.8$  and  $4.9 \pm 2.6$   $\phi K^+K^-$  events observed from the  $\psi(3770)$  resonance data and the continuum data. In the fits, the width of  $\phi$  is fixed to  $4.26 \text{ MeV}/c^2$  [20], and the mass resolution is fixed to  $3 \text{ MeV}/c^2$  determined by Monte Carlo simulation. However, no obvious  $\phi$  signals are observed in the other figures. Selecting the events with  $M_{K^+K^-}$  in the  $\phi$  signal regions, we obtain 3(1) and 2(0) signal events for the  $\phi\pi^+\pi^-$  ( $\phi p\bar{p}$ ) final state from the  $\psi(3770)$  resonance data and the continuum data, respectively.

##### D. Candidates for $e^+e^- \rightarrow m(\pi^+\pi^-)n(K^+K^-)i(p\bar{p})\eta/\pi^0$

Figures 4 and 5 show the distributions of the  $\gamma\gamma$  combinations from the selected  $m(\pi^+\pi^-)n(K^+K^-)i(p\bar{p})\gamma\gamma$  events for studying  $e^+e^- \rightarrow 2(\pi^+\pi^-)\eta$ ,  $e^+e^- \rightarrow 2(\pi^+\pi^-)\pi^0$ ,  $e^+e^- \rightarrow K^+K^-\pi^+\pi^-\pi^0$ ,  $e^+e^- \rightarrow 2(K^+K^-)\pi^0$ ,  $e^+e^- \rightarrow p\bar{p}\pi^0$ ,  $e^+e^- \rightarrow p\bar{p}\pi^+\pi^-\pi^0$  and  $e^+e^- \rightarrow 3(\pi^+\pi^-)\pi^0$ . In most of the figures, the sig-

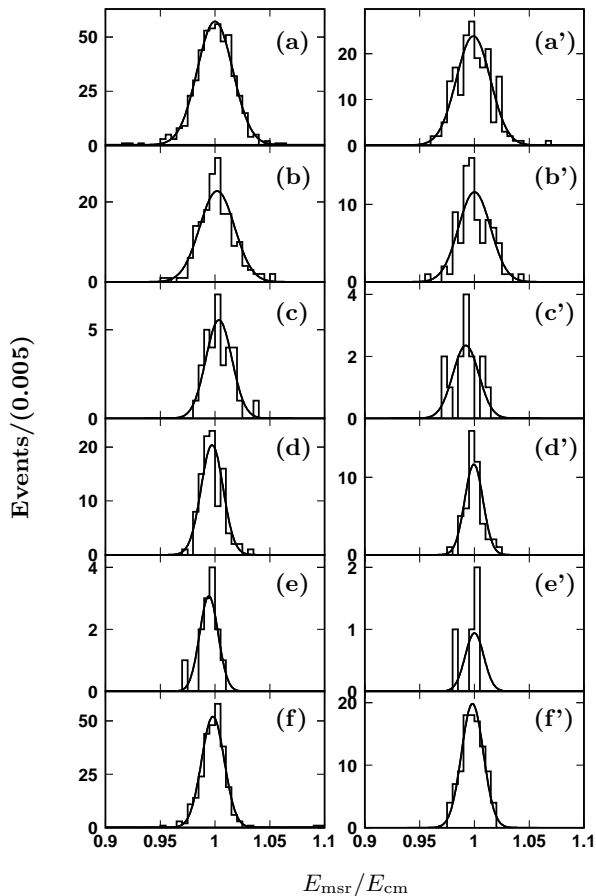


FIG. 2: The  $E_{\text{msr}}/E_{\text{cm}}$  distributions of the candidates for (a)  $e^+e^- \rightarrow 2(\pi^+\pi^-)$ , (b)  $e^+e^- \rightarrow K^+K^-\pi^+\pi^-$ , (c)  $e^+e^- \rightarrow 2(K^+K^-)$ , (d)  $e^+e^- \rightarrow p\bar{p}\pi^+\pi^-$ , (e)  $e^+e^- \rightarrow p\bar{p}K^+K^-$  and (f)  $e^+e^- \rightarrow 3(\pi^+\pi^-)$  selected from the  $\psi(3770)$  resonance data (left) and the continuum data (right).

nals for  $\eta/\pi^0$  production are clearly observed. Fitting to these  $\gamma\gamma$  invariant mass spectra with a Gaussian function for the  $\eta/\pi^0$  signal and a polynomial for the background yields the number  $N^{\text{obs}}$  of the signal events for each mode observed from the  $\psi(3770)$  resonance data and the continuum data. In the fits to the  $\gamma\gamma$  invariant mass spectra in Figs. 4(b), 5(d), 5(d') and 5(e'), the mass and the mass resolution of  $\eta/\pi^0$  are fixed to its nominal mass [20] and  $\sigma_{M_{\gamma\gamma}}^{\eta/\pi^0}$  determined by Monte Carlo simulation, respectively. However, there are only a few events in Figs. 5(c) and 5(c'). Selecting the events with  $M_{\gamma\gamma}$  in the  $\pi^0$  signal region, we obtain 6 and 0 signal events for the  $2(K^+K^-)\pi^0$  final state from the  $\psi(3770)$  resonance data and the continuum data, respectively.

## V. BACKGROUND SUBTRACTION

For some light hadron final states observed from the two data sets, there are the contributions from  $J/\psi$  and  $\psi(3686)$  decays, the contributions from the other final states due to misidentifying a  $\pi$  as  $K$  or reverse, and the contributions from  $D\bar{D}$  decays. The number of these con-

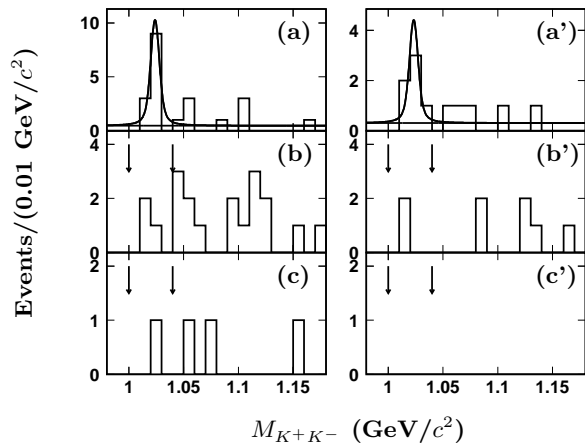


FIG. 3: The distributions of the invariant masses of the  $K^+K^-$  combinations from the candidates for (a)  $e^+e^- \rightarrow \phi K^+K^-$ , (b)  $e^+e^- \rightarrow \phi\pi^+\pi^-$  and (c)  $e^+e^- \rightarrow \phi p\bar{p}$  selected from the  $\psi(3770)$  resonance data (left) and the continuum data (right), where the pairs of arrows represent the  $\phi$  signal regions.

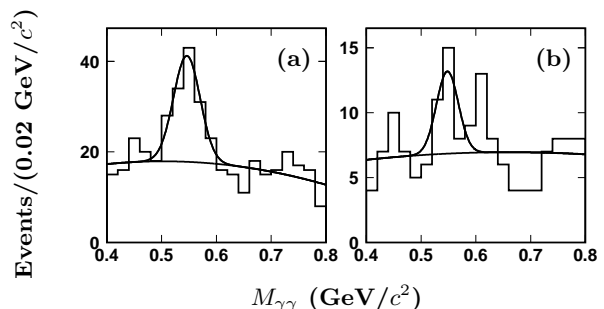


FIG. 4: The distributions of the invariant masses of the  $\gamma\gamma$  combinations from the candidates for  $e^+e^- \rightarrow 2(\pi^+\pi^-)\eta$  selected from (a) the  $\psi(3770)$  resonance data and (b) the continuum data.

tributions should be subtracted from the number  $N^{\text{obs}}$  of the candidate events for  $e^+e^- \rightarrow f$  ( $f$  represents light hadron final state). These are estimated by Monte Carlo simulation.

### A. Contributions from $J/\psi$ decays

The number of the contributions from the decay  $J/\psi \rightarrow f$ , where  $J/\psi$  is produced due to ISR returns, is estimated by

$$N_{J/\psi \rightarrow f} = \sigma_{J/\psi} \times \mathcal{L} \times \epsilon_{J/\psi \rightarrow f} \times \mathcal{B}(J/\psi \rightarrow f), \quad (1)$$

where  $\sigma_{J/\psi}$  is the cross section for  $J/\psi$  production determined with the  $J/\psi$  resonance parameters [20],  $\mathcal{L}$  is the integrated luminosity of the data set,  $\epsilon_{J/\psi \rightarrow f}$  is the detection efficiency obtained by analyzing the Monte Carlo

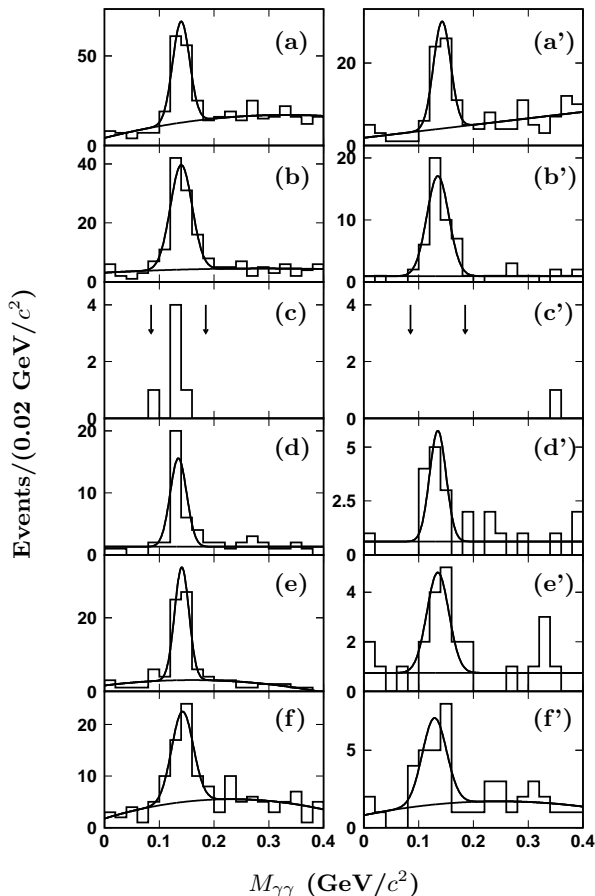


FIG. 5: The distributions of the invariant masses of the  $\gamma\gamma$  combinations from the candidates for (a)  $e^+e^- \rightarrow 2(\pi^+\pi^-)\pi^0$ , (b)  $e^+e^- \rightarrow K^+K^-\pi^+\pi^-\pi^0$ , (c)  $e^+e^- \rightarrow 2(K^+K^-)\pi^0$ , (d)  $e^+e^- \rightarrow p\bar{p}\pi^0$ , (e)  $e^+e^- \rightarrow p\bar{p}\pi^+\pi^-\pi^0$  and (f)  $e^+e^- \rightarrow 3(\pi^+\pi^-)\pi^0$  selected from the  $\psi(3770)$  resonance data (left) and the continuum signal data (right), where the pairs of arrows represent the  $\pi^0$  signal regions.

events of  $J/\psi \rightarrow f$ ,  $\mathcal{B}(J/\psi \rightarrow f)$  is the branching fraction for the decay  $J/\psi \rightarrow f$  [20].

### B. Contributions from $\psi(3686)$ decays

The estimate of the contributions from the decay  $\psi(3686) \rightarrow f$  is similarly done with Eq. (1) by substituting  $J/\psi$  with  $\psi(3686)$ . Here, the cross section  $\sigma_{\psi(3686)}$  for  $\psi(3686)$  production is determined with the  $\psi(3686)$  resonance parameters measured by BES Collaboration [5].

The number of the contributions from the decay  $\psi(3686) \rightarrow J/\psi\pi^+\pi^- \rightarrow f$  is estimated by

$$\begin{aligned}
 N_{\psi(3686) \rightarrow J/\psi\pi^+\pi^- \rightarrow f} &= \sigma_{\psi(3686)} \times \mathcal{L} \\
 &\times \epsilon_{\psi(3686) \rightarrow J/\psi\pi^+\pi^-, J/\psi \rightarrow f'} \\
 &\times \mathcal{B}(\psi(3686) \rightarrow J/\psi\pi^+\pi^-) \\
 &\times \mathcal{B}(J/\psi \rightarrow f'), \quad (2)
 \end{aligned}$$

where  $\epsilon_{\psi(3686) \rightarrow J/\psi\pi^+\pi^-, J/\psi \rightarrow f'}$  is the detection efficiency obtained by analyzing the Monte Carlo events of  $\psi(3686) \rightarrow J/\psi\pi^+\pi^-$  with  $J/\psi \rightarrow f'$ ,  $\mathcal{B}(\psi(3686) \rightarrow J/\psi\pi^+\pi^-)$  and  $\mathcal{B}(J/\psi \rightarrow f')$  are the branching fractions for the decays  $\psi(3686) \rightarrow J/\psi\pi^+\pi^-$  and  $J/\psi \rightarrow f'$  [20], respectively.

Monte Carlo study shows that the contributions from the decays  $\psi(3686) \rightarrow J/\psi\pi^0\pi^0$ ,  $\psi(3686) \rightarrow J/\psi\pi^0$ ,  $\psi(3686) \rightarrow J/\psi\eta$ ,  $\psi(3686) \rightarrow \gamma\chi_{cJ}$  ( $J = 0, 1, 2$ ) can be negligible.

### C. Cross background from the other final states

The events from the other final state  $e^+e^- \rightarrow i$  may be misidentified as the final state  $e^+e^- \rightarrow f$  in question. For example, the final states  $K^+K^-\pi^+\pi^-$  and  $2(\pi^+\pi^-)\pi^0$  may be faked as  $2(\pi^+\pi^-)$  due to misidentifying  $K^+K^-$  pair as  $\pi^+\pi^-$  pair and due to missing  $\pi^0$ . The number of these background events from  $e^+e^- \rightarrow i$  to  $e^+e^- \rightarrow f$  is estimated by

$$N_{\text{CB}} = \sigma_{e^+e^- \rightarrow i} \times \mathcal{L} \times \epsilon_{i \rightarrow f}, \quad (3)$$

where  $\sigma_{e^+e^- \rightarrow i}$  is the observed cross section for the final state  $e^+e^- \rightarrow i$ ,  $\epsilon_{i \rightarrow f}$  is the rate of misidentifying  $e^+e^- \rightarrow i$  as  $e^+e^- \rightarrow f$ .

### D. Contributions from $D\bar{D}$ decays

In the  $\psi(3770)$  resonance region, the events from  $D\bar{D}$  decays may also satisfy the selection criteria for the light hadron final states. The number of these events is estimated by analyzing a Monte Carlo sample which is about 78 times larger than the  $\psi(3770)$  resonance data. The Monte Carlo events are generated as  $e^+e^- \rightarrow D\bar{D}$ , where the  $D$  and  $\bar{D}$  mesons are set to decay into all possible final states with the branching fractions quoted from PDG [20]. The number of events satisfying the selection criteria for  $e^+e^- \rightarrow f$  in question is then normalized to the data, resulting in the number  $N_{D\bar{D}}$  of the contributions from  $D\bar{D}$  decays to  $e^+e^- \rightarrow f$ .

Monte Carlo study shows that the contributions from the decays  $\psi(3770) \rightarrow J/\psi\pi^+\pi^-$ ,  $\psi(3770) \rightarrow J/\psi\pi^0\pi^0$ ,  $\psi(3770) \rightarrow J/\psi\pi^0$ ,  $\psi(3770) \rightarrow J/\psi\eta$ ,  $\psi(3770) \rightarrow \gamma\chi_{cJ}$  ( $J = 0, 1, 2$ ) can be negligible.

### E. Number of signal events

Adding  $N_{J/\psi}$ ,  $N_{\psi(3686)}$ ,  $N_{\text{CB}}$  and  $N_{D\bar{D}}$  yields the total number  $N^{\text{b}}$  of the background events for each final state. After subtracting  $N^{\text{b}}$  from  $N^{\text{obs}}$ , we obtain the numbers  $N^{\text{net}}$  of the signal events for some final states, under the assumption that there is no interference between the light hadron final states of the resonance decays and those from the continuum production. For the other final states

with a few events observed from the data, we set the upper limits  $N^{\text{up}}$  on these numbers of the signal events by using the Feldman–Cousins method [21] in the absence of background at 90% confidence level (C.L.). The second, third and fourth columns of Tabs I and II summarize the results on the numbers  $N^{\text{obs}}$ ,  $N^{\text{b}}$  and  $N^{\text{net}}$  (or  $N^{\text{up}}$ ).

## VI. RESULTS

### A. Monte Carlo efficiency

The detection efficiency  $\epsilon$  for each final state is estimated by Monte Carlo simulation for the BESII detector [22]. The Monte Carlo events are generated by using a phase space generator including initial state radiation and photon vacuum polarization corrections [23] with  $1/s$  cross section energy dependence. Final state radiation [24] decrease the detection efficiency not more than 0.5%. Detailed analysis gives the detection efficiency for each final state at  $\sqrt{s} = 3.773$  and 3.650 GeV. They are summarized in the fifth columns of Tabs. I and II. For the modes containing  $\phi$ ,  $\pi^0$  and  $\eta$  mesons in the final states, the detection efficiencies listed in the tables do not include the branching fractions for the decays  $\phi \rightarrow K^+K^-$ ,  $\pi^0 \rightarrow \gamma\gamma$  and  $\eta \rightarrow \gamma\gamma$ .

### B. Systematic error

In the measurements of the observed cross sections for  $e^+e^- \rightarrow$  light hadrons, the systematic error arises mainly from the uncertainties in luminosity ( $\sim 2.1\%$  [4, 5]), photon selection ( $\sim 2.0\%$  per photon), tracking efficiency ( $\sim 2.0\%$  per track), particle identification ( $\sim 0.5\%$  per pion or kaon,  $\sim 2.0\%$  per proton), kinematic fit ( $\sim 1.5\%$ ), Monte Carlo statistics ( $\sim (1.1\sim 3.2)\%$ ), branching fractions quoted from PDG [20] ( $\sim 1.22\%$  for  $\mathcal{B}(\phi \rightarrow K^+K^-)$ ,  $\sim 0.03\%$  for  $\mathcal{B}(\pi^0 \rightarrow \gamma\gamma)$  and  $\sim 0.66\%$  for  $\mathcal{B}(\eta \rightarrow \gamma\gamma)$ ), background subtraction ( $\sim (0.0\sim 4.8)\%$ ), fit to mass spectrum ( $\sim 3.8\%$ ), and Monte Carlo modeling ( $\sim 6.0\%$ ). Adding these uncertainties in quadrature yields the total systematic error  $\Delta_{\text{sys}}$  for each final state at  $\sqrt{s} = 3.773$  and 3.650 GeV, respectively, which are shown in the sixth columns of Tabs. I and II.

### C. Observed cross sections for some final states

The observed cross section for  $e^+e^- \rightarrow f$  is determined by

$$\sigma = \frac{N^{\text{net}}}{\mathcal{L} \times \epsilon [\times \mathcal{B}(\phi \rightarrow K^+K^-)] [\times \mathcal{B}(\pi^0/\eta \rightarrow \gamma\gamma)]}, \quad (4)$$

where  $N^{\text{net}}$  is the number of the signal events,  $\epsilon$  is the detection efficiency for the final state, and  $\mathcal{B}(\phi \rightarrow K^+K^-)$  and  $\mathcal{B}(\pi^0/\eta \rightarrow \gamma\gamma)$  are the branching fractions for the

decays  $\phi \rightarrow K^+K^-$  and  $\pi^0/\eta \rightarrow \gamma\gamma$  [20], respectively. Inserting these numbers in Eq. (4), we obtain the observed cross sections for some final states at  $\sqrt{s} = 3.773$  and 3.650 GeV, respectively. They are shown in the last columns of Tabs. I and II, where the first error is statistical and the second systematic. The measured observed cross sections for  $e^+e^- \rightarrow 3(\pi^+\pi^-)$  and  $e^+e^- \rightarrow K^+K^-\pi^+\pi^-\pi^0$  at  $\sqrt{s} = 3.650$  GeV are consistent with the results in Refs. [25, 26] within error.

### D. Upper limits on the observed cross sections for the other final states

The upper limit on the observed cross section for  $e^+e^- \rightarrow f$  with a few events observed from the data is set by

$$\sigma^{\text{up}} = \frac{N^{\text{up}}}{\mathcal{L} \times \epsilon \times (1 - \Delta_{\text{sys}}) [\times \mathcal{B}(\phi \rightarrow K^+K^-)] [\times \mathcal{B}(\pi^0/\eta \rightarrow \gamma\gamma)]}, \quad (5)$$

where  $N^{\text{up}}$  is the upper limit on the number of the signal events, and  $\Delta_{\text{sys}}$  is the systematic error in the measurement of the observed cross section for the final state. Inserting the corresponding numbers in Eq. (5), we obtain the upper limits on the observed cross sections for these final states at  $\sqrt{s} = 3.773$  and 3.650 GeV, respectively, which are also shown in the last columns of Tabs. I and II. The upper limits on the observed cross sections for  $e^+e^- \rightarrow \phi\pi^0$  and  $e^+e^- \rightarrow \phi\eta$  are consistent with the measurements [13] from the CLEO Collaboration.

### E. Upper limits on the observed cross section and the branching fraction for $\psi(3770) \rightarrow f$

If we don't consider the interference effects between the continuum and resonance amplitudes, we may calculate the observed cross section for  $\psi(3770) \rightarrow f$  by

$$\sigma_{\psi(3770) \rightarrow f} = \sigma_{e^+e^- \rightarrow f}^{3.773 \text{ GeV}} - f_{\text{co}} \times \sigma_{e^+e^- \rightarrow f}^{3.650 \text{ GeV}}, \quad (6)$$

where  $\sigma_{e^+e^- \rightarrow f}^{3.773 \text{ GeV}}$  and  $\sigma_{e^+e^- \rightarrow f}^{3.650 \text{ GeV}}$  are the measured observed cross sections for  $e^+e^- \rightarrow f$  at 3.773 and 3.650 GeV, respectively, and  $f_{\text{co}}$  is the coefficient due to the  $1/s$  dependence of the cross section. The results on  $\sigma_{\psi(3770) \rightarrow f}$  are shown in the second column of Tab. III, where the first error is statistical, the second is the independent systematic, and the third is the common systematic error. Here, the independent systematic error is from the uncertainties in the Monte Carlo statistics, in fitting to the mass spectrum and in the background subtraction, while the common systematic error is from the other uncertainties as discussed in the subsection B. For the final states of  $\phi\pi^0$ ,  $\phi\eta$ ,  $\phi\pi^+\pi^-$ ,  $\phi p\bar{p}$  and  $2(K^+K^-)\pi^0$ , only a few signal events are observed from both the  $\psi(3770)$

TABLE I: The observed cross sections for  $e^+e^- \rightarrow$  light hadrons at  $\sqrt{s} = 3.773$  GeV, where  $N^{\text{obs}}$  is the number of events observed from the  $\psi(3770)$  resonance data,  $N^{\text{b}}$  is the total number of background events,  $N^{\text{net}}$  is the number of the signal events,  $N^{\text{up}}$  is the upper limit on the number of the signal events,  $\epsilon$  is the detection efficiency for the final state,  $\Delta_{\text{sys}}$  is the relative systematic error in the measurement of the observed cross section,  $\sigma$  is the observed cross section and  $\sigma^{\text{up}}$  is the upper limit on the observed cross section set at 90% C.L..

$e^+e^- \rightarrow$	$N^{\text{obs}}$	$N^{\text{b}}$	$N^{\text{net}}$ (or $N^{\text{up}}$ )	$\epsilon$ [%]	$\Delta_{\text{sys}}$ [%]	$\sigma$ (or $\sigma^{\text{up}}$ ) [pb]
$\phi\pi^0$	0	0	$< 2.44$	$9.08 \pm 0.14$	8.9	$< 3.5$
$\phi\eta$	1	0	$< 4.36$	$11.31 \pm 0.16$	8.9	$< 12.6$
$2(\pi^+\pi^-)$	$462.5 \pm 21.9$	$7.8 \pm 1.0$	$454.7 \pm 21.9$	$15.13 \pm 0.18$	10.6	$173.7 \pm 8.4 \pm 18.4$
$K^+K^-\pi^+\pi^-$	$181.0 \pm 13.5$	$4.9 \pm 0.6$	$176.1 \pm 13.5$	$7.73 \pm 0.13$	10.7	$131.7 \pm 10.1 \pm 14.1$
$\phi\pi^+\pi^-$	3	0	$< 7.42$	$8.81 \pm 0.13$	10.7	$< 11.1$
$2(K^+K^-)$	$33.0 \pm 5.8$	$1.1 \pm 0.2$	$31.9 \pm 5.8$	$9.26 \pm 0.14$	10.6	$19.9 \pm 3.6 \pm 2.1$
$\phi K^+K^-$	$12.1 \pm 3.9$	$0.1 \pm 0.0$	$12.0 \pm 3.9$	$8.94 \pm 0.14$	11.4	$15.8 \pm 5.1 \pm 1.8$
$p\bar{p}\pi^+\pi^-$	$103.0 \pm 10.2$	$4.0 \pm 0.4$	$99.0 \pm 10.2$	$17.26 \pm 0.19$	11.5	$33.2 \pm 3.4 \pm 3.8$
$p\bar{p}K^+K^-$	$13.0 \pm 3.7$	$0.2 \pm 0.0$	$12.8 \pm 3.7$	$10.48 \pm 0.14$	11.6	$7.1 \pm 2.0 \pm 0.8$
$\phi p\bar{p}$	1	0	$< 4.36$	$9.96 \pm 0.14$	11.6	$< 5.8$
$3(\pi^+\pi^-)$	$268.7 \pm 16.5$	$3.8 \pm 0.6$	$264.9 \pm 16.5$	$6.47 \pm 0.11$	14.1	$236.7 \pm 14.7 \pm 33.4$
$2(\pi^+\pi^-)\eta$	$71.4 \pm 18.6$	$0.1 \pm 0.1$	$71.3 \pm 18.6$	$6.81 \pm 0.12$	12.0	$153.7 \pm 40.1 \pm 18.4$
$2(\pi^+\pi^-)\pi^0$	$110.2 \pm 14.4$	$26.5 \pm 2.7$	$83.7 \pm 14.4$	$6.05 \pm 0.11$	12.4	$80.9 \pm 13.9 \pm 10.0$
$K^+K^-\pi^+\pi^-\pi^0$	$88.3 \pm 12.6$	$5.3 \pm 0.7$	$83.0 \pm 12.6$	$2.83 \pm 0.08$	12.2	$171.6 \pm 26.0 \pm 20.9$
$2(K^+K^-)\pi^0$	$6.0 \pm 2.5$	$0.1 \pm 0.1$	$5.9 \pm 2.5$	$1.91 \pm 0.06$	11.8	$18.1 \pm 7.7 \pm 2.1$
$p\bar{p}\pi^0$	$26.8 \pm 5.7$	$0.7 \pm 0.1$	$26.1 \pm 5.7$	$15.12 \pm 0.18$	10.3	$10.1 \pm 2.2 \pm 1.0$
$p\bar{p}\pi^+\pi^-\pi^0$	$50.4 \pm 8.3$	$2.3 \pm 0.4$	$48.1 \pm 8.3$	$5.30 \pm 0.11$	12.9	$53.1 \pm 9.2 \pm 6.8$
$3(\pi^+\pi^-)\pi^0$	$43.6 \pm 10.1$	$12.5 \pm 1.5$	$31.1 \pm 10.1$	$1.72 \pm 0.04$	16.0	$105.8 \pm 34.4 \pm 16.9$

TABLE II: The observed cross sections for  $e^+e^- \rightarrow$  light hadrons at  $\sqrt{s} = 3.650$  GeV, where  $N^{\text{obs}}$  is the number of events observed from the continuum data, and the definitions of the other symbols are the same as those in Tab. I.

$e^+e^- \rightarrow$	$N^{\text{obs}}$	$N^{\text{b}}$	$N^{\text{net}}$ (or $N^{\text{up}}$ )	$\epsilon$ [%]	$\Delta_{\text{sys}}$ [%]	$\sigma$ (or $\sigma^{\text{up}}$ ) [pb]
$\phi\pi^0$	0	0	$< 2.44$	$9.48 \pm 0.14$	8.9	$< 8.9$
$\phi\eta$	0	0	$< 2.44$	$11.82 \pm 0.16$	8.9	$< 18.0$
$2(\pi^+\pi^-)$	$185.2 \pm 13.7$	$1.9 \pm 0.3$	$183.3 \pm 13.7$	$15.87 \pm 0.18$	10.6	$177.7 \pm 13.3 \pm 18.8$
$K^+K^-\pi^+\pi^-$	$85.0 \pm 9.3$	$0.9 \pm 0.1$	$84.1 \pm 9.3$	$8.00 \pm 0.13$	10.6	$161.7 \pm 17.9 \pm 17.1$
$\phi\pi^+\pi^-$	2	0	$< 5.91$	$9.08 \pm 0.13$	10.7	$< 22.9$
$2(K^+K^-)$	$14.0 \pm 3.8$	0	$14.0 \pm 3.8$	$8.94 \pm 0.13$	10.6	$24.1 \pm 6.5 \pm 2.6$
$\phi K^+K^-$	$4.9 \pm 2.6$	0	$4.9 \pm 2.6$	$8.81 \pm 0.14$	11.4	$17.4 \pm 9.2 \pm 2.0$
$p\bar{p}\pi^+\pi^-$	$49.0 \pm 7.0$	$0.8 \pm 0.1$	$48.2 \pm 7.0$	$17.60 \pm 0.19$	11.5	$42.1 \pm 6.1 \pm 4.8$
$p\bar{p}K^+K^-$	$4.0 \pm 2.0$	0	$4.0 \pm 2.0$	$10.03 \pm 0.14$	11.6	$6.1 \pm 3.1 \pm 0.7$
$\phi p\bar{p}$	0	0	$< 2.44$	$9.49 \pm 0.14$	11.6	$< 9.1$
$3(\pi^+\pi^-)$	$99.0 \pm 10.0$	$0.2 \pm 0.0$	$98.8 \pm 10.0$	$6.47 \pm 0.11$	14.1	$234.9 \pm 23.8 \pm 33.1$
$2(\pi^+\pi^-)\eta$	$15.9 \pm 7.4$	0	$15.9 \pm 7.4$	$7.17 \pm 0.13$	12.0	$86.6 \pm 40.3 \pm 10.4$
$2(\pi^+\pi^-)\pi^0$	$51.0 \pm 8.5$	$2.3 \pm 0.4$	$48.7 \pm 8.5$	$6.10 \pm 0.11$	12.0	$124.3 \pm 21.7 \pm 14.9$
$K^+K^-\pi^+\pi^-\pi^0$	$40.5 \pm 6.8$	$0.3 \pm 0.1$	$40.2 \pm 6.8$	$2.81 \pm 0.08$	12.2	$222.8 \pm 37.7 \pm 27.2$
$2(K^+K^-)\pi^0$	0	0	$< 2.44$	$1.87 \pm 0.06$	11.7	$< 23.0$
$p\bar{p}\pi^0$	$9.7 \pm 3.5$	$0.1 \pm 0.0$	$9.6 \pm 3.5$	$16.19 \pm 0.19$	10.3	$9.2 \pm 3.4 \pm 1.0$
$p\bar{p}\pi^+\pi^-\pi^0$	$10.1 \pm 3.8$	$0.2 \pm 0.1$	$9.9 \pm 3.8$	$5.31 \pm 0.11$	12.9	$29.0 \pm 11.1 \pm 3.7$
$3(\pi^+\pi^-)\pi^0$	$15.5 \pm 5.5$	$0.7 \pm 0.1$	$14.8 \pm 5.5$	$1.82 \pm 0.04$	15.2	$126.6 \pm 47.1 \pm 19.2$

resonance data and the continuum data, therefore we neglect their contributions from the continuum production.

The upper limits on the observed cross sections for  $\psi(3770)$  decay to  $\phi\pi^0$ ,  $\phi\eta$ ,  $\phi\pi^+\pi^-$  and  $\phi p\bar{p}$  are directly set based on the upper limits on their observed cross sections at 3.773 GeV. However, the upper limits on the observed cross sections for  $\psi(3770)$  decay to the other final states are set by shifting the cross section by  $1.64\sigma$ , where the  $\sigma$  is the total error of the measured cross section. If the central value of  $\sigma_{\psi(3770)\rightarrow f}$  is less than zero, we treat it as zero, then we set its upper limit. The third column of Tab. III summarizes the results on  $\sigma_{\psi(3770)\rightarrow f}^{\text{up}}$ .

BES Collaboration measured the observed cross section for the  $\psi(3770)$  production at  $\sqrt{s} = 3.773$  GeV to be  $6.94 \pm 0.48 \pm 0.28$  nb [5] and  $7.25 \pm 0.27 \pm 0.34$  nb [28] with two different data samples. Averaging these two results, we obtain the weighted average cross section  $\sigma_{\psi(3770)}^{\text{obs}} = 7.15 \pm 0.27 \pm 0.27$  nb, where the first error is the combined statistical and independent systematic error, and the second is the common systematic error of the two measurements. The upper limit on the branching fraction  $\mathcal{B}_{\psi(3770)\rightarrow f}^{\text{up}}$  for  $\psi(3770) \rightarrow f$  is set by dividing  $\sigma_{\psi(3770)\rightarrow f}^{\text{up}}$  by  $\sigma_{\psi(3770)}^{\text{obs}}$ . The fourth column of Tab. III summarizes the results on  $\mathcal{B}_{\psi(3770)\rightarrow f}^{\text{up}}$ .

## VII. SUMMARY

In summary, using the data sets collected at  $\sqrt{s} = 3.773$  and 3.650 GeV with the BESII detector at the BEPC collider, we have measured the observed cross sections for 18 exclusive light hadron final states produced in  $e^+e^-$  annihilation at the two energy points. These cross sections exclude the contributions from  $J/\psi$ ,  $\psi(3686)$  and  $D\bar{D}$  decays. The initial state radiation and photon vacuum polarization corrections are taken into account in

the determination of the detection efficiency. In the measurements we do not consider the interference effects between the continuum and resonance amplitudes, since we do not know the details about the two amplitudes. For this reason, although we do not observe significant difference between the observed cross sections for most light hadron final states at the two energy points, we can not draw a conclusion that the  $\psi(3770)$  does not decay into these final states. To extract the branching fractions for  $\psi(3770) \rightarrow$  light hadrons from the observed cross sections, one needs to collect large data samples at more different energy points, i.e. cross section scan, covering both  $\psi(3770)$  and  $\psi(3686)$  [27]. This will hopefully be done with the coming BESIII detector at the BEPCII collider in the near future. However, the measurements of the observed cross sections for these light hadron final states at the two energy points provide useful information to understand the mechanisms of the continuum light hadron production and still provide valuable information to understand the discrepancy between the observed cross sections for  $D\bar{D}$  and  $\psi(3770)$  production.

## VIII. ACKNOWLEDGMENTS

The BES collaboration thanks the staff of BEPC for their hard efforts. This work is supported in part by the National Natural Science Foundation of China under contracts Nos. 10491300, 10225524, 10225525, 10425523, the Chinese Academy of Sciences under contract No. KJ 95T-03, the 100 Talents Program of CAS under Contract Nos. U-11, U-24, U-25, the Knowledge Innovation Project of CAS under Contract Nos. U-602, U-34 (IHEP), the National Natural Science Foundation of China under Contract No. 10225522 (Tsinghua University).

- 
- [1] DELCO Collaboration, W. Bacino et al., Phys. Rev. Lett. **40** (1978) 671.
  - [2] G. Rong, D. H. Zhang, J. C. Chen, hep-ex/0506051.
  - [3] J. L. Rosner, hep-ph/0405196, submitted to Phys. Rev. D.
  - [4] BES Collaboration, M. Ablikim et al., Phys. Lett. **B 641** (2006) 145.
  - [5] BES Collaboration, M. Ablikim et al., Phys. Rev. Lett. **97** (2006) 121801.
  - [6] BES Collaboration, J. Z. Bai et al., HEP & NP **28(4)** (2004) 325.
  - [7] BES Collaboration, M. Ablikim et al., Phys. Lett. **B 605** (2005) 63.
  - [8] BES Collaboration, M. Ablikim et al., Phys. Rev. **D 70** (2004) 077101.
  - [9] BES Collaboration, M. Ablikim et al., Phys. Rev. **D 72** (2005) 072007.
  - [10] CLEO Collaboration, N. E. Adam et al., Phys. Rev. Lett. **96** (2006) 082004.
  - [11] CLEO Collaboration, T. E. Coans et al., Phys. Rev. Lett. **96** (2006) 182002.
  - [12] CLEO Collaboration, G. S. Huang et al., Phys. Rev. Lett. **96** (2006) 032003.
  - [13] CLEO Collaboration, G. S. Adams et al., Phys. Rev. **D 73** (2006) 012002.
  - [14] CLEO Collaboration, D. Cronin-Hennessy et al., Phys. Rev. **D 74** (2006) 012005.
  - [15] CLEO Collaboration, R. A. Briere et al., Phys. Rev. **D 74** (2006) 031106.
  - [16] BES Collaboration, J. Z. Bai et al., Nucl. Instrum. Methods **A 344** (1994) 319.
  - [17] BES Collaboration, J. Z. Bai et al., Nucl. Instrum. Methods **A 458** (2001) 627.
  - [18] BES Collaboration, M. Ablikim et al., Phys. Lett. **B 597** (2004) 39; Phys. Lett. **B 603** (2004) 130; Phys. Lett. **B 608** (2005) 24.
  - [19] BES Collaboration, M. Ablikim et al., Nucl. Phys. **B 727** (2005) 395.
  - [20] Particle Data Group, W.-M. Yao, et al., J. Phys. **G 33** (2006) 1.



TABLE III: The upper limits on the observed cross section  $\sigma_{\psi(3770)\rightarrow f}^{\text{up}}$  and the branching fraction  $\mathcal{B}_{\psi(3770)\rightarrow f}^{\text{up}}$  for  $\psi(3770) \rightarrow f$  are set at 90% C.L.. The  $\sigma_{\psi(3770)\rightarrow f}$  in the second column is calculated with Eq. (6), where the first error is the statistical, the second is the independent systematic, and the third is the common systematic error. Here, the upper <sup>t</sup> denotes that we treat the upper limit on the observed cross section for  $e^+e^- \rightarrow f$  at 3.773 GeV as  $\sigma_{\psi(3770)\rightarrow f}^{\text{up}}$ , the upper <sup>n</sup> denotes that we neglect the contribution from the continuum production, and the upper <sup>z</sup> denotes that we treat the central value of  $\sigma_{\psi(3770)\rightarrow f}$  as zero if it is less than zero.

Decay Mode	$\sigma_{\psi(3770)\rightarrow f}$ [pb]	$\sigma_{\psi(3770)\rightarrow f}^{\text{up}}$ [pb]	$\mathcal{B}_{\psi(3770)\rightarrow f}^{\text{up}}$ [ $\times 10^{-3}$ ]
$\phi\pi^0$	$< 3.5^{tn}$	$< 3.5$	$< 0.5$
$\phi\eta$	$< 12.6^{tn}$	$< 12.6$	$< 1.9$
$2(\pi^+\pi^-)$	$7.4 \pm 15.0 \pm 2.8 \pm 0.8$	$< 32.5$	$< 4.8$
$K^+K^-\pi^+\pi^-$	$-19.6 \pm 19.6 \pm 3.3 \pm 2.1^z$	$< 32.7$	$< 4.8$
$\phi\pi^+\pi^-$	$< 11.1^{tn}$	$< 11.1$	$< 1.6$
$2(K^+K^-)$	$-2.7 \pm 7.1 \pm 0.5 \pm 0.3^z$	$< 11.6$	$< 1.7$
$\phi K^+K^-$	$-0.5 \pm 10.0 \pm 0.9 \pm 0.1^z$	$< 16.5$	$< 2.4$
$p\bar{p}\pi^+\pi^-$	$-6.2 \pm 6.6 \pm 0.6 \pm 0.7^z$	$< 11.0$	$< 1.6$
$p\bar{p}K^+K^-$	$1.4 \pm 3.5 \pm 0.1 \pm 0.2$	$< 7.2$	$< 1.1$
$\phi p\bar{p}$	$< 5.8^{tn}$	$< 5.8$	$< 0.9$
$3(\pi^+\pi^-)$	$16.9 \pm 26.7 \pm 5.5 \pm 2.4$	$< 61.7$	$< 9.1$
$2(\pi^+\pi^-)\eta$	$72.7 \pm 55.0 \pm 7.3 \pm 8.2$	$< 164.7$	$< 24.3$
$2(\pi^+\pi^-)\pi^0$	$-35.4 \pm 24.6 \pm 6.6 \pm 4.0^z$	$< 42.3$	$< 6.2$
$K^+K^-\pi^+\pi^-\pi^0$	$-36.9 \pm 43.8 \pm 12.8 \pm 4.2^z$	$< 75.2$	$< 11.1$
$2(K^+K^-)\pi^0$	$18.1 \pm 7.7 \pm 0.7 \pm 2.0^n$	$< 31.2$	$< 4.6$
$p\bar{p}\pi^0$	$1.5 \pm 3.9 \pm 0.5 \pm 0.1$	$< 7.9$	$< 1.2$
$p\bar{p}\pi^+\pi^-\pi^0$	$26.0 \pm 13.9 \pm 2.6 \pm 3.2$	$< 49.7$	$< 7.3$
$3(\pi^+\pi^-)\pi^0$	$-12.7 \pm 55.9 \pm 8.7 \pm 1.8^z$	$< 92.8$	$< 13.7$

- [21] G. J. Felman and R. D. Cousins, Phys. Rev. **D 57** (1998) 3873.
- [22] BES Collaboration, M. Ablikim et al., Nucl. Instrum. Methods **A 552** (2005) 344.
- [23] E. A. Kuraev and V. S. Fadin, Yad. Fiz. **41** (1985) 733.
- [24] E. Barberio, Z. Was, Comput. Phys. Commun. **79** (1994) 291.
- [25] BES Collaboration, M. Ablikim et al., Phys. Rev. **D 72** (2005) 012002.
- [26] BES Collaboration, M. Ablikim et al., Phys. Rev. **D 73** (2005) 052004.
- [27] G. Rong (For BES Collaboration), Int. J. Mod. Phys. **A 21** (2006) 5416.
- [28] BES Collaboration, M. Ablikim et al., hep-ex/0612056.